77-22

The Transmission of Acoustic Plane Waves at a Jet Exhaust

Robert H. Schlinker*
United Technologies Research Center, East Hartford, Conn.

An experimental study was conducted to determine the plane-wave acoustic transmission loss at the exit of an unflanged constant diameter circular duct with subsonic flow. This model geometry simulated the physical conditions at an engine exhaust in the simplest manner. Higher-order acoustic modes were not considered since at typical core-noise frequencies these modes are usually cut off and therefore decay before reaching the nozzle exit. The acoustic transmission coefficient was evaluated over a large range of jet Mach numbers and reduced frequencies. Results show that the plane-wave mode component of internal noise is transmitted at the duct exit interface with minimal attenuation at the high Mach numbers relevant to engine operating conditions.

Nomenclature

A	= downstream propagating wave amplitude
a	= duct radius
B	= upstream propagating wave amplitude
c_0	= sound speed
G	= microphone sensitivity
H	= cross-correlation peak amplitude
I	= intensity of propagating acoustic waves
i	= complex number, $i=(-1)^{1/2}$
K	= wave number
M_1, M_2	= in-duct Mach number and forward flight Mach number
P	= pressure
R	= duct exit pressure reflection coefficient
r	= radial duct coordinate
S	= cross-correlation function
t	= time
V	= voltage
x	= axial duct coordinate
α	= duct exit acoustic energy transmission coefficient
α'	= predicted duct exit acoustic energy transmission coefficient
β	= location of first maximum in cross-correlation time trace
γ_a, γ_b	= constants defined by Eqs. (20) and (21)
Δ	= difference operator
ϵ	= cut-on wave number for first higher-order mode
μ	= constant defined by Eq. (19)
τ	= delay time
ϕ	= phase angle
ω	= frequency, rad/s
$\langle\ \rangle$	= time average
$\lvert\ \rvert$	= absolute value

Subscripts, Superscripts

c	= combined signal consisting of acoustic standing wave and boundary-layer pressure fluctuations
d	= acoustic driver signal
sw	= acoustic standing wave signal
T	= turbulent boundary-layer fluctuations
$+, -$	= downstream and upstream propagating waves
1, 2	= axial stations 1 and 2
$\sim$	= complex parameter
$*$	= complex conjugate

Presented as Paper 77-22 at the AIAA 15th Aerospace Sciences Meeting, Los Angeles, Calif., Jan. 24-26, 1977; submitted June, 1977; revision received Sept. 21, 1978.

Index categories: Aeroacoustics; Noise.

*Research Engineer, Aeroacoustics and Experimental Gas Dynamics Group. Member AIAA.

Introduction

Objective

A KNOWLEDGE of the acoustic transmission losses between the combustor and the engine far field is a prerequisite to reducing core-engine noise. Prediction schemes exist for calculating the magnitude of the losses associated with the combustor/duct coupling and the turbine.[1] However, the losses across the duct termination must also be known before far-field core-engine noise levels can be calculated. The present experimental study conducted at model scale, addresses this question.

The objective of the study was to determine the acoustic transmission loss at the exit of an unflanged circular duct with subsonic flow present. The study was restricted to plane-wave noise incident at the duct exhaust. Higher-order modes were not considered since at typical core-noise frequencies these modes are usually cut off and therefore decay before reaching the nozzle exit. By using a constant diameter duct and limiting the study to plane-wave internal noise, a simple but reasonable approximation to the actual physical conditions at an engine exhaust was investigated.

Previous Investigations

As shown by the analysis in the present study, the plane-wave duct exit transmission coefficient can be deterimined once the pressure reflection coefficient is known. For this reason, considerable emphasis was placed on the reflection coefficient in the present study. A discussion of previous investigations in this area is thus warranted.

Levine and Schwinger[2] developed a theory which determined the duct exit pressure reflection coefficient for the case of a plane wave with no flow using an unflanged constant diameter duct model. Carrier[3] extended the theoretical work of Levine to include the effect of flow in the duct. He employed continuity of transverse acoustic particle velocity as a boundary condition at the shear layer interface between the uniform jet exhaust flow and the ambient air. It is presently accepted that the transverse acoustic particle displacement should be continuous[4-6] as indicated in Fig. 1.

Mani[6] also investigated the effect of Mach number on the pressure reflection coefficient. His analysis, limited to a two-dimensional duct, used continuity of acoustic particle displacement as a boundary condition. Savkar[7] developed a general theory for spinning acoustic modes incident on a circular duct termination with a flow mismatch between the jet exhaust and the freestream. Continuity of transverse particle velocity and particle displacement were applied separately as boundary conditions at the shear layer interface. Sample calculations were presented for the special case of a plane wave incident at the duct exhaust. The objective was to

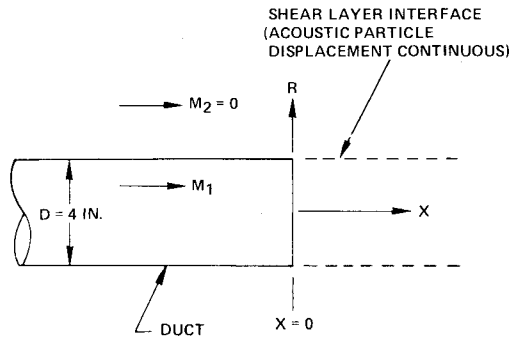

Fig. 1 Geometry of unflanged duct termination acoustic transmission study.

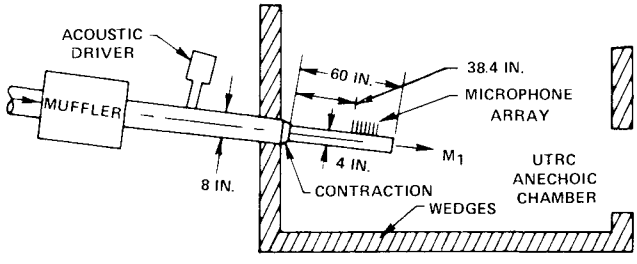

Fig. 2 Plan view of duct test apparatus.

determine which boundary condition best predicted existing experimental plane-wave results. Unfortunately, the small difference in the calculated results failed to provide a critical assessment of the two boundary conditions.

Another treatment of the reflection coefficient for plane waves and higher-order modes may be found in the work of Lansing.[8] In addition to accounting for the reflection of individual modes, the theory calculates the conversion coefficients which describe the energy converted from the mth mode to the nth reflected mode. However, the analysis considered only a uniform freestream with $M_1 = M_2$.

A more recent treatment of the plane-wave reflection coefficient for a circular duct was provided by Wahbah and Strahle.[9] The results, applicable to flows with a temperature mismatch between the jet and the surroundings, were limited to low Mach numbers.

While the theory has been slow in evolving, the experimental measurements of relevant model problems have also been limited in number. Among the measurements available are those of Mechel et al.[10] and Ronneberger[11] who determined the plane-wave reflection coefficient for a baffled duct termination at low Mach numbers. Such measurements are difficult due to the inadequacy of acoustic instrumentation for use in turbulent flow.

Description of the Experiment

The configuration treated here is depicted in Fig. 1. The model consisted of a uniform straight duct of diameter D with rigid impervious walls and an unflanged duct termination. A jet flow of nearly uniform subsonic Mach number M_1 issued from the circular duct. The region $r > D/2$ was occupied by still air ($M_2 = 0$) at approximately the same temperature as the jet. Tests were limited to cold flows because of the difficulty of making microphone measurements with heated flow.

Several Mach numbers were considered during the study. $M_1 = 0$ was used to verify the experimental techniques for measuring the duct transmission coefficient. The results were compared to the existing theory of Levine and Schwinger.[2] Higher Mach numbers, $M_1 = 0.25$ and 0.43, were selected to simulate engine operating conditions during landing approach when combustion noise is significant. Finally, $M_1 = 0.70$ was added to the test matrix to provide a complete evaluation of the transmission characteristics with increasing Mach number.

The present study was conducted in the United Technologies Research Center Acoustic Research Tunnel. A schematic of the duct test apparatus is shown in Fig. 2. Air was supplied from a high-pressure line through a muffler and a plenum to the 4-in. constant diameter duct test section. An acoustic driver, located in the plenum, generated the periodic plane-wave mode used to simulate core-engine noise. The jet and sound exhausted into an anechoic chamber.

As shown by the analysis discussed subsequently, the duct exit transmission coefficient is determined once the internal reflection is known. The latter parameter is customarily evaluated by generating a steady-state standing wave field in the duct. The acoustic pressure field is then measured by means of a microphone probe which moves along the axis of the tube. The reflection coefficient is calculated from the amplitudes of the pressure maxima and minima in the wave pattern.

The preceding method was initially evaluated to determine if it could be applied to the present problem with flow in the duct. It was concluded that the in-flow microphone self-noise level and flow noise generated by the traversing equipment dominated the harmonic signal generated by the acoustic driver. In addition, the downstream wake generated by the microphone and traversing equipment would destroy the uniform duct flow.

A different measurement technique for the preceding experimental approach was therefore developed as part of the present investigation. Flush-mounted wall microphones were located at different axial stations along the duct to measure the standing wave amplitudes generated by the acoustic driver. The individual microphone signals were cross-correlated with the periodic input signal to the acoustic driver. The purpose of the correlations was to remove the random boundary-layer pressure fluctuations sensed by the microphones. The resulting correlation technique did not require probing the standing wave acoustic pressure field for the maxima stations in the duct.

Having considered the basic concepts involved in the present experiment, the details can now be described. A discrete frequency tone was introduced into an 8-in-diam pipe (see Fig. 2) from an acoustic driver situated 12-ft upstream of the duct exit. The resulting standing wave in the duct downstream of the contraction was measured by seven ¼-in. diam, flush-mounted, wall microphones. By using an array of microphones, the spacing between microphone pairs could be selected to permit analyzing standing wave patterns with vastly different wavelengths. The farthest downstream microphone was 10 in. from the duct exit.

The upper frequency limit selected for each Mach number insured that only plane waves existed at the microphone measurement array. This was verified analytically[12] given the initial condition that all higher-order modes would be transmitted at the contraction between the 8-in. and 4-in. diam pipes. Based on the duct propagation characteristics in the 4-in.-diam pipe, it was shown that the acoustic pressure field decay rate was sufficient to ensure that only plane waves existed at the microphone array. The acoustic decay was also verified experimentally[12] at Mach numbers $M_1 = 0$ and 0.5 for frequencies not exceeding the analytically determined cut-on frequencies.

Analysis

Acoustic Energy Transmission Coefficient

With flow present in a duct, the intensity of the upstream and downstream propagating plane waves are known to be different. As shown by Morfey[13] and Amiet[14] for axial flow with no swirl, the intensity ratio is

$$\frac{I^-}{I^+} = \left(\frac{P^-}{P^+}\right)^2 \left(\frac{1-M_1}{1+M_1}\right)^2 \tag{1}$$

Here P^- and P^+ correspond to the pressure amplitudes of the upstream and downstream traveling waves, respectively.

Equation (1) can now be applied toward calculating the acoustic energy transmission coefficient α at the nozzle exit. By definition

$$\alpha = 1 - \frac{I^-}{I^+} = 1 - R^2\left(\frac{1-M_1}{1+M_1}\right)^2 \tag{2}$$

where $R = |P^-/P^+|$ is the pressure reflection coefficient at the jet exhaust.

Equation (2) indicates that the transmission coefficient is determined once the internal pressure reflection coefficient is known. The latter parameter was obtained using the experimental technique described in the previous section.

Pressure Reflection Coefficient

When a standing plane-wave system, with frequency ω, exists in a uniform duct flow, the forward and reflected pressure waves may be written in complex notation as (see Morfey[13]):

$$\tilde{P}^+(x,t) = \tilde{A}e^{i(\omega t - K^+ x)}, \quad K^+ = \frac{K}{1+M_1} \tag{3}$$

$$\tilde{P}^-(x,t) = \tilde{B}e^{i(\omega t + K^- x)}, \quad K^- = \frac{K}{1-M_1} \tag{4}$$

where $K = \omega/c_0$. The amplitude coefficients, $\tilde{A}$ and $\tilde{B}$, are in general complex constants for a plane wave.

The duct termination pressure reflection coefficient is represented by the absolute value of the complex ratio $\tilde{P}^-/\tilde{P}^+$. Thus, $R = |\tilde{P}^-/\tilde{P}^+| = |\tilde{B}|/|\tilde{A}|$. The pressure amplitudes, $\tilde{A}$ and $\tilde{B}$, can now be determined from the standing wave sound pressure $\tilde{P}_{sw}$ at any two axial stations. At location x_1,

$$\tilde{P}_{sw}(x_1,t) = \tilde{P}^+(x_1,t) + \tilde{P}^-(x_1,t) \tag{5}$$

The spatial and temporal dependence of the term on the left of Eq. (5) can be separated since the standing wave is periodic in x and t giving

$$\tilde{P}_1(x_1)e^{i\omega t} = \tilde{A}e^{i(\omega t - K^+ x_1)} + \tilde{B}e^{i(\omega t + K^- x_1)} \tag{6}$$

A similar equation can be written for $\tilde{P}_{sw}$ at any given station x_2 downstream of x_1.

Solving the system of two equations, $P_{sw}(x_1, t)$, $P_{sw}(x_2, t)$, for $|\tilde{A}|$, $|\tilde{B}|$ and noting that $x_2 = x_1 + \Delta x$ gives

$$|\tilde{A}| = \frac{|\tilde{P}_1 - \tilde{P}_2 e^{-iK^-\Delta x}|}{|e^{-ix_1(K^+ + K^-)} - e^{-ix_2(K^+ + K^-)}|}, \quad \Delta x = x_2 - x_1 > 0 \tag{7}$$

$$|\tilde{B}| = \frac{|\tilde{P}_1 - \tilde{P}_2 e^{+iK^+\Delta x}|}{|e^{ix_1(K^+ + K^-)} - e^{ix_2(K^+ + K^-)}|} \tag{8}$$

and

$$R = \left|\frac{\tilde{P}_1 - \tilde{P}_2 e^{iK^+\Delta x}}{\tilde{P}_1 - \tilde{P}_2 e^{-iK^-\Delta x}}\right| \tag{9}$$

A similar analysis was recently employed by Johnston and Schmidt[15] as part of a study to measure the reflection coefficients for flow through square-edged orifice plates. They expressed the reflection coefficient in terms of the absolute distances x_1 and x_2, where $x = 0$ corresponded to the origin of the coordinate system at the speaker. The authors indicated that the finite depth of the speaker cone created uncertainties in the values of x_1 and x_2. This problem was amplified as frequency increased because the acoustic wavelength decreased relative to the uncertainties in x_1 and x_2. The present formulation in Eq. (9) avoids this problem by using only the distance between the two microphone stations which can be measured accurately.

Measurement of Wave Amplitude

It now remains to evaluate the reflection coefficient in Eq. (9) using the measured microphone signals at each station. One approach, referred to as the autocorrelation technique and discussed in detail in Ref. 12, measures the autocorrelation amplitude at x_1 and the cross-correlation amplitude between the microphones at x_1, and x_2. The ability to measure the former term depends on the microphone signal-to-noise ratio. This term was successfully evaluated for $M_1 = 0$, but, with flow present, the periodic standing wave signal was masked by the boundary-layer pressure fluctuations also sensed by the microphone. Another approach was therefore employed to evaluate the standing wave signal.

The second method for extracting the standing wave pressure signal in Eq. (9) required cross correlating the measured microphone signal with the periodic acoustic driver signal. This technique was applied independently by Johnston and Schmidt.[15]

The net pressure signal sensed by a microphone at any given station is $P_c = P_{sw} + P_T$. Here P_T represents the turbulent boundary-layer pressure fluctuations. Note that P_c, P_{sw}, and P_T are real quantities, since they represent the measured signals.

The microphone output voltage is linearly related to the measured acoustic pressure signal by the microphone sensitivity G. Thus, the voltage signal from the microphone at the given axial location x_1 is $V_c(x_1, t) = GP_c(x_1, t)$. Similar expressions relating voltage and acoustic pressure exist for P_{sw}, P_T, P_1, and P_2.

Cross correlating the output voltage V_c with the periodic driver input voltage V_d and noting that the turbulent fluctuations are uncorrelated with the periodic signals gives the real function

$$S(x_1,\tau) = \langle V_d(t)\, V_{sw}(x_1, t+\tau)\rangle \tag{10}$$

If the harmonic signals for V_d and V_{sw} are expressed in terms of complex notation

$$V_d(t) = |V_d| \cos\omega t = \left|\frac{V_d}{2}\right|(e^{i\omega t} + e^{-i\omega t}) \tag{11}$$

and

$$V_{sw}(x_1, t+\tau) = \tfrac{1}{2}[\tilde{V}_1 e^{i\omega(t+\tau)} + \tilde{V}_1^* e^{-i\omega(t+\tau)}] \tag{12}$$

Substituting the expressions for V_d and V_{sw} in the equation for the cross correlation gives

$$S(x_1,\tau) = \tfrac{1}{2}[\tfrac{1}{2}|V_d|\tilde{V}_1^* e^{-i\omega\tau} + \tfrac{1}{2}|V_d|\tilde{V}_1 e^{i\omega\tau}] \tag{13}$$

In the present experiment the measured cross-correlation parameter $S(x_1, \tau)$ is a real function which is expected to be periodic with respect to τ. It can be represented by a peak amplitude, H_1 (real), and a phase ϕ_1, by which V_d leads V_1 at station x_1. Then,

$$S(x_1,\tau) = H_1 \cos(\omega\tau - \phi_1)$$

$$= \tfrac{1}{2}[H_1 e^{i(\omega\tau - \phi_1)} + H_1 e^{-i(\omega\tau - \phi_1)}] \tag{14}$$

Comparing like exponential terms in Eqs. (13) and (14)

$$\tilde{V}_1 = (2H_1 e^{-i\phi_1})/|V_d| \tag{15}$$

A similar expression can be obtained for $\tilde{V}_2$. Since $\tilde{P}_1$ and $\tilde{P}_2$ are linked to the voltage by the microphone sensitivity the final expression for the reflection coefficient is

$$R = \left| \frac{1-(H_2G_1/H_1G_2)e^{i(K^+\Delta x-\Delta\phi)}}{1-(H_2G_1/H_1G_2)e^{-i(K^-\Delta x+\Delta\phi)}} \right| \tag{16}$$

where

$$\Delta\phi = \phi_2 - \phi_1 = 2\pi(\beta_2 - \beta_1) \tag{17}$$

Here β is the cross-correlation delay expressed in cycles with $0 \le \beta \le 1$. Finally

$$R = \left[\frac{(1-\mu\cos\gamma_a)^2 + (\mu\sin\gamma_a)^2}{(1-\mu\cos\gamma_b)^2 + (\mu\sin\gamma_b)^2} \right]^{1/2} \tag{18}$$

$$\mu = \frac{H_2}{H_1}\frac{G_1}{G_2} \tag{19}$$

$$\gamma_a = K^+\Delta x - \frac{2\pi}{\omega}(\beta_2 - \beta_1) \tag{20}$$

$$\gamma_b = K^-\Delta x + \frac{2\pi}{\omega}(\beta_2 - \beta_1) \tag{21}$$

Results and Discussion

The measured pressure reflection coefficient for $M_1 = 0$ is plotted in Fig. 3 as a function of the reduced frequency, Ka. This nondimensional parameter, consisting of the wave number and the duct radius, has been shown analytically to be one of the parameters controlling duct exit reflections. The experiment was limited to $Ka < \epsilon$, where ϵ corresponds to the reduced frequency at which the next higher-order mode is cut on. For no-flow conditions, $\epsilon = 1.84$ as indicated in Fig. 3.

The results in Fig. 3 were obtained using the cross-correlation and autocorrelation techniques. The measurements closely agree with the theory for the unflanged open-ended duct problem treated by Levine and Schwinger. This indicates that the experimental technique adopted here is accurate. It also represents the first direct experimental verification of the Levine and Schwinger theory for unflanged ducts.

The pressure reflection coefficient for $M_1 = 0.25$ is shown in Fig. 4. The reflection coefficient in the presence of flow exceeded the no-flow value since the effect of flow is to increase the amplitude of upstream propagating waves relative to downstream propagating waves.[16] This is a physically acceptable result and does not invalidate conservation of acoustic energy requirements. To verify this, the intensity ratio of upstream (I^-) and downstream (I^+) propagating acoustic waves was evaluated using Eq. (1). The calculated result, plotted in Fig. 4, indicates $(I^-/I^+)^{1/2} \le 1$ at all reduced frequencies.

Figure 5 summarizes the effect of Mach number on the pressure reflection coefficient. The curves represent a mean line through the data points associated with each Mach number. For example, the solid line drawn through the $M_1 = 0.25$ data points in Fig. 4 is repeated in Fig. 5

Experimental support for the present results is provided by the study of Mechel et al. who reported measurements of the plane-wave pressure reflection coefficient for a baffled opening. Figure 6 compares the present unflanged duct measurements at $M_1 = 0.25$ with their results at approximately the same Mach number. Good agreement exists at low reduced frequencies, but the flanged geometry results are lower at large Ka.

Exact agreement between experimental results in Fig. 6 cannot be expected due to the different duct termination geometries. The importance of the exit geometry is illustrated in Fig. 7 using the theoretical results for the $M_1 = 0$ case. Here the pressure reflection coefficient for the flanged geometry is smaller at all reduced frequencies. This is similar to the trend observed at high reduced frequencies in Fig. 6.

The pressure reflection coefficient for $M_1 = 0.43$ in Fig. 5 can also be compared to the flanged duct exit measurements obtained by Ronneberger at $M_1 = 0.4$. For the reduced

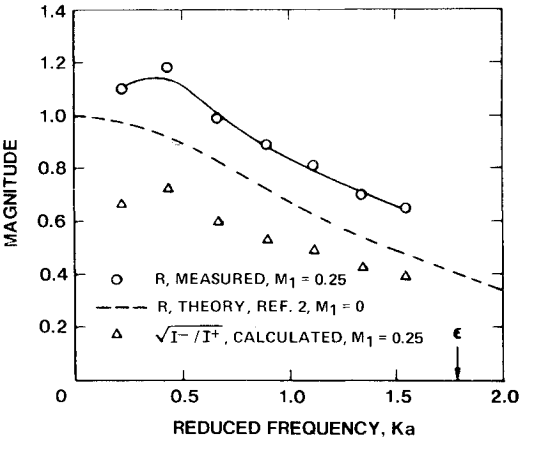

Fig. 4 Pressure and intensity reflection coefficients for unflanged termination, $M_1 = 0.25$.

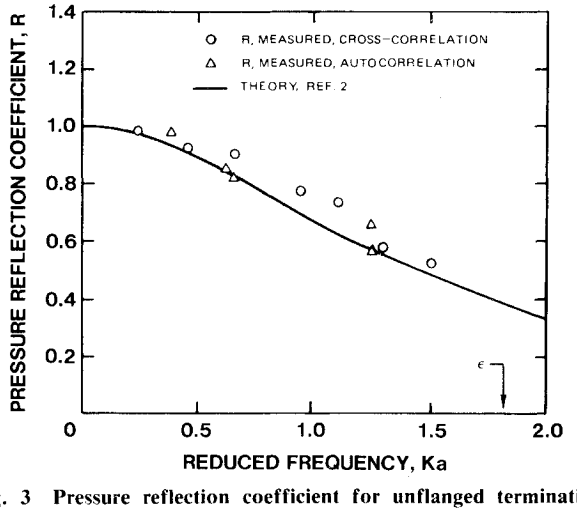

Fig. 3 Pressure reflection coefficient for unflanged termination, $M_1 = 0$.

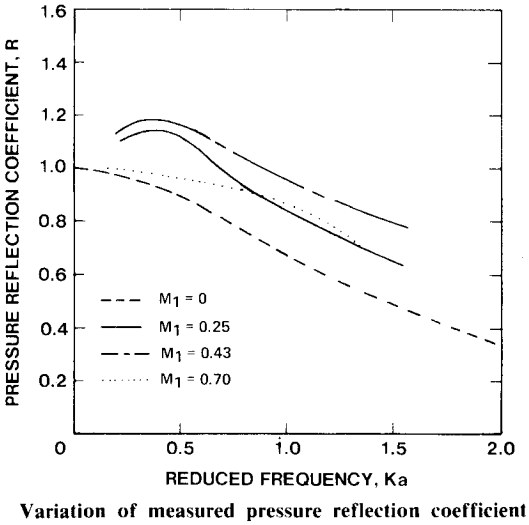

Fig. 5 Variation of measured pressure reflection coefficient with Mach number for unflanged termination.

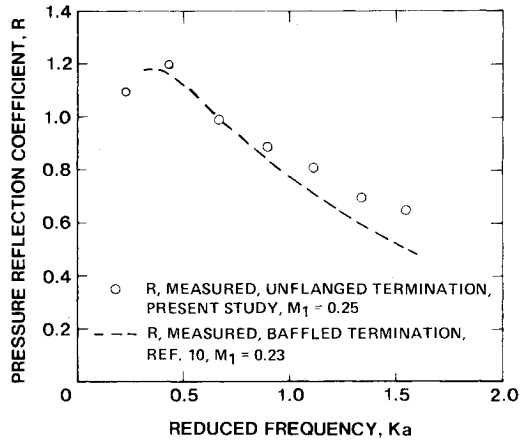

Fig. 6 Pressure reflection coefficient for unflanged and baffled terminations, $M_f \approx 0.25$.

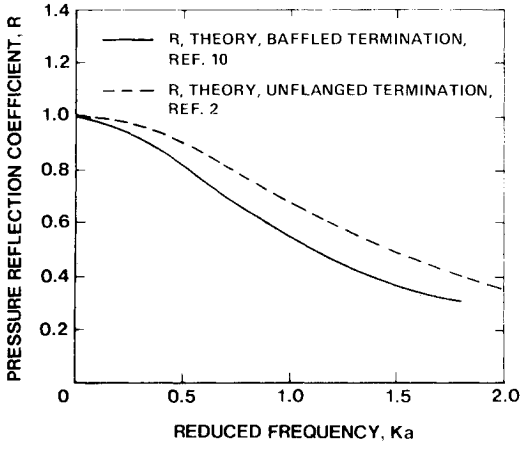

Fig. 7 Pressure reflection coefficient for unflanged and baffled terminations, $M_f = 0$.

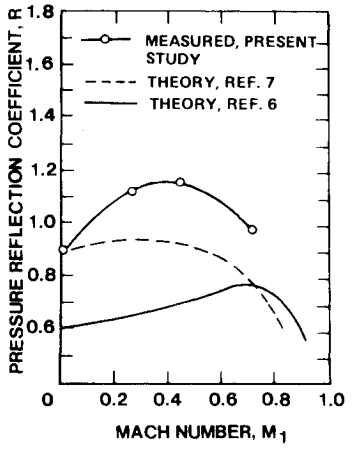

Fig. 8 Effect of Mach number on pressure reflection coefficient at $Ka = 0.50$.

frequency range, $0.25 \leq Ka \leq 1$, the magnitude of the pressure reflection coefficient is approximately the same for the two different duct exit geometries. In particular, both studies indicte a reflection coefficient greater than unity, which is similar to the result obtained at $M = 0.25$. Comparisons at larger reduced frequencies are not possible since Ronneberger limted his study to $Ka \leq 1$.

Figure 8 demonstrates the effect of Mach number on the pressure reflection coefficient at a fixed reduced frequency, $Ka = 0.5$. The theory of Savkar using the continuous particle displacement is compared with the experimental results of the present study. Both curves show a maximum at approximately

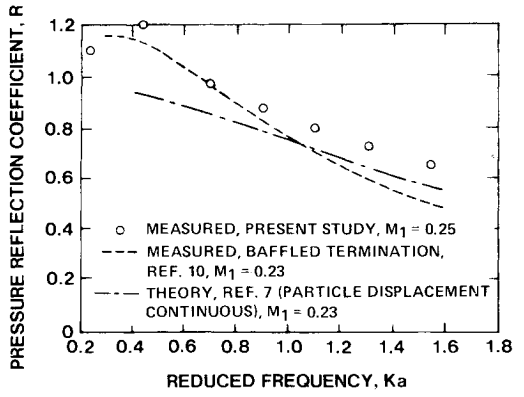

Fig. 9 Effect of reduced frequency on pressure reflection coefficient, $M_f \approx 0.25$.

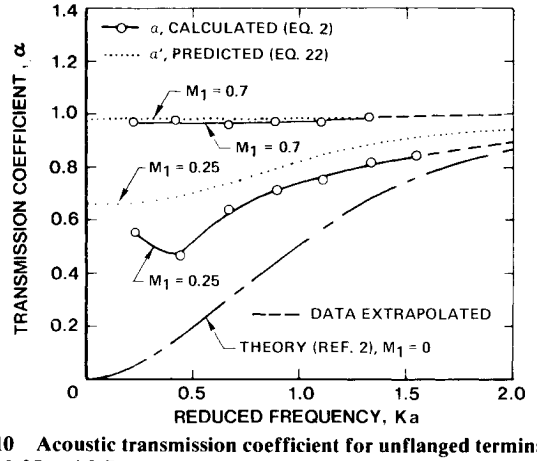

Fig. 10 Acoustic transmission coefficient for unflanged termination, $M_f = 0.25$ and 0.7.

the same Mach number, but the absolute values differ. Thus, the Savkar analysis may be helpful for calculating trends, although additional improvements are needed before predicted values agree with experimental results.

Mani also investigated the effect of Mach number on the pressure reflection coefficient. His theoretical analysis, limited to a two dimensional duct, also used the continuous acoustic particle displacement boundary condition. Comparison of his two-dimensional analysis (based on the equation on p. 512 of his report) with the present circular duct measurements indicates a significant difference (see Fig. 8) between the two geometries. Consequently, the two-dimensional theory cannot be expected to predict the circular duct pressure reflection coefficient. However, the two geometries do exhibit larger reflection coefficients in the presence of flow. It should be noted that the two-dimensional duct width was represented by the circular duct diameter in the calculation shown in Fig. 8.

Figure 9 provides a comparison of the experimental and calculated reflection coefficients as a function of reduced frequency for a fixed Mach number, $M_f = 0.25$. The theoretical curve was calculated by Savkar. While there is good agreement at large reduced frequency, the theory is unable to predict the measured coefficient at small Ka. In particular, it fails to predict a reflection coefficient greater than unity. This is similar to the theory-experiment disagreement in Fig. 8.

The theory of Carrier was not included in the comparisons shown in Figs. 8 and 9 since he employed continuity of transverse acoustic particle velocity as a boundary condition at the shear layer interface. It is presently accepted[4-6] that the transverse acoustic particle displacement should be continuous. Also, the complicated analytical expressions obtained by Carrier did not facilitate numerical calculations.

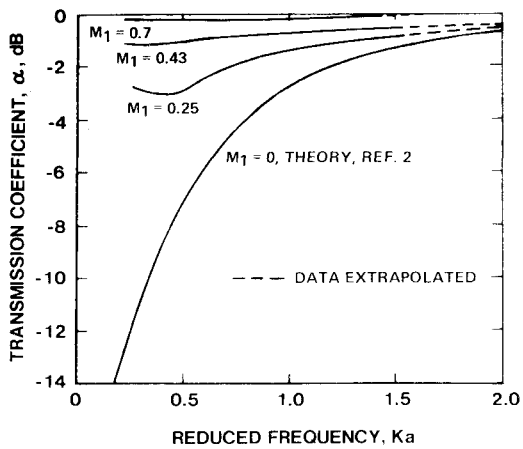

Fig. 11 Variation of measured acoustic transmission coefficient with Mach number for unflanged termination.

Once the pressure reflection coefficient is known, the acoustic energy transmission coefficient α can be calculated using Eq. (2). Figure 10 shows the calculated results based on the corresponding measured reflection coefficients for two of the Mach numbers in Fig. 5. In each case, the presence of flow increased the transmission coefficient relative to the no-flow condition.

The variation of the transmission coefficient with increasing Mach number is summarized in Fig. 11. Tests without flow indicate a sizeable exit plane impedance mismatch which causes the duct to act as a high-pass filter since the plane-wave transmission coefficient increases with frequency. The primary effect of flow is to minimize the impedance mismatch and eliminate the high-pass filter characteristics. This effect is exemplified by the transmission coefficient approaching unity (0 dB) at all frequencies as Mach number increases. Based on this result, the plane-wave mode component of core-engine noise would be expected to be transmitted without significant attenuation at the jet exhaust.

An analytical technique for predicting the transmission coefficient in Fig. 11 would be desirable. One approach would be to use the analysis of Savkar to calculate the reflection coefficient needed to determine the transmission coefficient from Eq. (2). However, the amplitude discrepancy between the reflection coefficients obtained by Savkar and the present experimental results (see Figs. 8 and 9) suggests that the Savkar analysis is unsatisfactory.

An alternate approach was therefore developed to predict the transmission coefficient with flow present. Using the reflection coefficient corresponding to $M_J = 0$, the transmission coefficient was approximated by

$$\alpha'(M_J) = 1 - R^2(M_J = 0)\left(\frac{1 - M_J}{1 + M_J}\right)^2 \qquad (22)$$

The predicted results are shown in Fig. 10 (and Figs. 13-15) in Ref. 12) for two Mach numbers. For $M_J = 0.25$, the calculated and measured values differ by 20%, but, at the higher Mach number the difference becomes negligible.

The good agreement with increasing Mach number occurs because the second term on the right-hand side of Eq. (22) approaches zero rapidly. This trend is dominated by the parameter $(1 - M_J^2/1 + M_J)^2$ suggesting that the precise value of R at a particular Mach number is not needed. The product, $R^2(1 - M_J)^2/(1 + M_J)^2$, is always small relative to unity so that minor variations in R can be tolerated. This explains why $R^2(M_J = 0)$ may be used in place of $R^2(M_J)$ to calculate the acoustic transmission coefficient when M_J becomes large.

It should be noted that the present experimental results are limited to the interface of a constant diameter duct. Although this test geometry represents a simple approximation to the true physical situation at a jet exhaust, it does not account for additional reflections across the variable area of a contracting nozzle nor any attenuation which may occur due to propagation through the jet shear layer.

Conclusions

Tests conducted without flow show good agreement between the measured pressure reflection coefficient and existing theories for an unflanged circular duct opening. Thus, the experimental technique developed as part of the present study is accurate. The principal conclusions obtained with this method in the presence of flow may be summarized as follows:

1) The pressure reflection coefficient in the presence of flow exceeds the no-flow value. The coefficient assumes values greater than unity without invalidating conservation of acoustic energy requirements in the duct. For a fixed reduced frequency the coefficient initially increases in the range $0 \leq M_J \leq 0.43$ after which it decreases.

2) The reflection coefficient for unflanged and flanged duct terminations are similar at small reduced frequencies.

3) The existing theory of Savkar is capable of predicting trends but not magnitudes of the reflection coefficient at large reduced frequencies.

4) The acoustic transmission coefficient approaches unity at all frequencies as the Mach number increases. Thus, while the reflected pressure amplitude can exceed the incident amplitude, acoustic energy is still transmitted with minimal attenuation across the duct exit interface.

5) The transmission coefficient for high subsonic Mach numbers is adequately predicted with an approximate equation.

Acknowledgment

This study was sponsored by Pratt and Whitney Aircraft Group, Commercial Products Division, United Technologies Corporation. The author acknowledges numerous helpful discussions with his colleague, R.K. Amiet.

References

[1] Mathews, D.C. and Rekos, N.F., Jr., "Prediction and Measurement of Direct Combustion Noise Turbopropulsion Systems," *Journal of Aircraft*, Vol. 14, Sept. 1977, pp. 850-859.

[2] Levine, H. and Schwinger, J., "On the Radiation of Sound from an Unflanged Circular Pipe," *Physical Review*, Vol. 73, Feb. 1948, pp. 383-406.

[3] Carrier, G.F., "Sound Transmission from a Tube With Flow," *Quarterly of Applied Mathematics*, Vol. 13, Jan. 1956, pp. 457-461.

[4] Ribner, H.S., "Reflection Transmission and Amplification of Sound by a Moving Medium," *Journal of the Acoustical Society of America*, Vol. 29, Apr. 1957, pp. 435-441

[5] Gottlieb, P., "Sound Source Near a Velocity Discontinuity," *Journal of the Acoustical Society of America*, Vol. 32, Sept. 1960, pp. 1117-1122.

[6] Mani, R., "Refraction of Acoustic Duct Waveguide Modes by Exhaust Jets," *Quarterly of Applied Mathematics*, Vol. 30, Jan. 1973, pp. 501-520.

[7] Savkar, S.D., "Radiation of Cylindrical Duct Acoustic Modes with Flow Mismatch," *Journal of Sound and Vibration*, Vol. 42, Oct. 1975, pp. 363-386.

[8] Lansing, D.L., Drischler, J.A., and Pusey, C.G., "Radiation of Sound From an Unflanged Circular Duct with Flow," Presented at the 79th Meeting of the Acoustical Society of America, Atlantic City, N.J., 1970.

[9]Wahbah, M. and Strahle, W.C., "Sound Radiation from a Duct for the Case of Low Mach Number," *AIAA Journal,* Vol. 15, April 1977, pp. 553-560.

[10]Mechel, F., Schilz, W., and Dietz, J., "Akustische Impedanz Einer Luftdurchstromten Offnung," *Acustica,* Vol. 15, Oct. 1965, pp. 199-206.

[11]Ronnaberger, D., "Experimentelle Untersuchungen zum akustischen Reflexionsfaktor von unstetigen Querschnittsanderungen in einem luftdurchstromten Rohr," *Acustica,* Vol. 19, Oct. 1967/1968, pp. 222-235.

[12]Schlinker, R.H., "The Transmission of Acoustic Plane Waves at a Jet Exhaust," AIAA Paper 77-22, Los Angeles, Calif., Jan. 24-26 1977.

[13]Morfey, C.L., "Sound Transmission and Generation in Ducts with Flow," *Journal of Sound and Vibration,* Vol. 14, Jan. 1971, pp. 37-55.

[14]Amiet, R.K., "Sound Produced by Singularities in an Annulus with Flow," United Technologies Research Center, East Hartford, Conn., Rept. 621866-1, 1972.

[15]Johnston, J.P. and Schmidt, W.E., "Measurement of Acoustic Reflection from an Obstruction in a Pipe with Flow," *Journal of the Acoustical Society of America,* Vol. 63, May 1978, pp. 1455-1460.

[16]Ingard, U. and Singhal, V., "Upstream and Downstream Sound Radiation into a Moving Fluid," *Journal of the Acoustical Society of America,* Vol. 54, Nov. 1973, pp. 1343-1346.